ELSEVIER

Contents lists available at ScienceDirect

# Journal of Molecular Spectroscopy

journal homepage: www.elsevier.com/locate/yjmsp



# Laboratory rotational spectroscopy of the magnesium-carbon chains $\rm MgC_4H$ and $\rm MgC_3N$



P. Bryan Changala a,\*, Nadav Genossar-Dan b, Joshua H. Baraban b, Michael C. McCarthy a

- <sup>a</sup> Center for Astrophysics | Harvard & Smithsonian, Cambridge, MA, 02138, USA
- <sup>b</sup> Department of Chemistry, Ben-Gurion University of the Negev, Beer Sheva, 8410501, Israel

#### ARTICLE INFO

Keywords: Rotational spectroscopy Metal-ligand molecules Astrochemistry Laser-coolable molecules

#### ABSTRACT

Recent advances in circumstellar metal chemistry and laser-coolable molecules have spurred interest in the spectroscopy and electronic properties of alkaline earth metal-bearing polyatomic molecules. We report the microwave rotational spectra of two members of this important chemical family, the linear magnesium-carbon chains  $MgC_4H$  and  $MgC_3N$ , detected with cavity Fourier transform microwave spectroscopy of a laser ablation-electric discharge expansion. The rotation, fine, and hyperfine parameters have been derived from the precise laboratory rest frequencies. These experimental results, combined with a theoretical quantum chemical analysis, confirm the recent identification of  $MgC_4H$  and  $MgC_3N$  in the circumstellar envelope of the evolved carbon-rich star IRC+10216. The spectroscopic data also provide insight into the structural and electronic properties that influence the metal-based optical cycling center in this unique class of laser-coolable polyatomics.

#### 1. Introduction

Radio astronomical observations of the evolved carbon-rich star IRC+10216 have revealed a rich metal chemistry in its inner layers and circumstellar shell. Equilibrium and non-equilibrium processes are thought to produce a large number of gas-phase molecules with highly ionic metal-ligand bonds, including small cyanides, isocyanides and acetylides [1-10]. Of these, the magnesium-carbon chains and clusters are by far the most extensively characterized family of metal-bearing circumstellar molecules. The identification of  $Mg(CC)_nH$ ,  $Mg(CC)_{n-1}$ (NC/CN), and HMg(CC)<sub>n-1</sub>(NC/CN) chains up to n = 3 [7,8,10–14]; their positively charged ions with n = 2-3 [15]; and the cyclic MgC<sub>2</sub> metal dicarbide [16] in IRC+10216 provides strong support for an ion-molecule radiative association-dissociative recombination pathway that incorporates metal atoms into polyatomic molecules in the circumstellar shell [17-19]. Although an extensive literature of optical laboratory data exists for many of these Mg-bearing species [20-27], high resolution microwave/mm-wave laboratory spectra are known only for the smallest members: MgCCH [28-31], MgCN/MgNC/HMgNC [7, 11,32-34], and MgC<sub>2</sub> [16]. The astronomical identification of the longer-chain molecules by radio detection has therefore relied primarily on quantum chemical calculations [13-15], motivating a renewed effort to produce these species in the laboratory and measure their rotational rest frequencies to high accuracy.

Motivated by these astrophysical and fundamental considerations, we have produced  $MgC_4H$  and  $MgC_3N$  in the laboratory with a laser ablation-electric discharge supersonic expansion source and detected their rotational spectra with a sensitive cavity Fourier transform microwave (FTMW) spectrometer. The precise spectroscopic constants derived from the laboratory rest frequencies are consistent with those derived from recent astronomical observations [13]. When combined with

E-mail address: bryan.changala@cfa.harvard.edu (P.B. Changala).

Alkaline earth metal-containing molecules are also of fundamental interest in molecular physics. Ionic monovalent metal-ligand compounds (ML, with L = OH, OCH3, CCH, etc.) are the most common polyatomic candidates for direct laser-cooling applications because of the unique electronic structure of the unpaired electron localized on the metal atom [35,36]. This optically active electron interacts only weakly with the rest of the molecule, giving rise to quasi-atomic metal-centered electronic excitations with highly diagonal vibrational Franck-Condon factors, which are necessary for efficient photon cycling schemes. Metal acetylides are intriguing laser-cooling candidates in this class because they can potentially accommodate multiple metal atoms whose interactions can be tuned by simply elongating the chain with repeated C=C units, i.e.,  $M-(CC)_n-M'$  [37,38]. Quantifying the precise structural and electronic properties of long alkaline-earth metal-carbon chains is therefore crucial to illuminating the chemical design principles of these complex laser-coolable polyatomics [30].

Corresponding author.

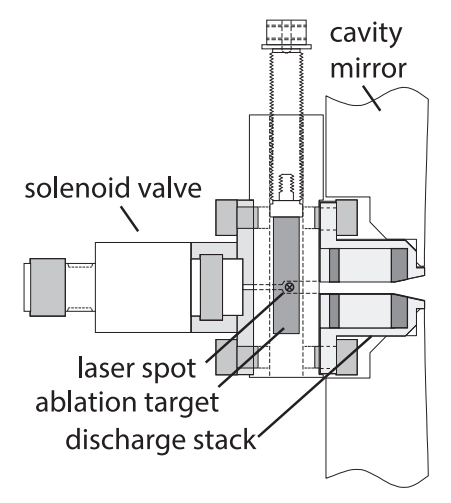


**Fig. 1.** Laser ablation-electric discharge expansion source. A solenoid valve releases a pulse of precursor gas mixture synchronized with a laser pulse that ablates a rotating cylindrical metal target positioned outside the valve. The entrained ablation products continue through a stack of discharge electrodes and supersonically expand into the vacuum microwave cavity.

a variety of additional laboratory assays and tests, and new theoretical calculations, these measurements confirm beyond any reasonable doubt the identification of  $MgC_4H$  and  $MgC_3N$  in IRC+10216. A comparison of the structural and electronic properties inferred from their rotational, fine, and hyperfine parameters with those of the shorter analogues (e.g., MgCCH and MgCN) provides insight into the chemical and electronic trends of this important family of metal-ligand molecules.

#### 2. Experimental

MgC<sub>4</sub>H and MgC<sub>3</sub>N were produced in a laser ablation-electric discharge expansion source at conditions similar to those of other closelyrelated alkaline earth metal-bearing molecules recently studied in our laboratory, including MgCCH [30] and MgC<sub>2</sub> [16] (see Fig. 1). A dilute mixture of organic precursors in neon (~0.1% acetylene, diacetylene, or acetonitrile) was expanded into a large vacuum chamber through a pulsed solenoid valve operating at a 5 Hz repetition rate with a ~500 µs pulse length. After the gas exits the valve, it passes a rotating magnesium rod that was ablated by a 5 ns, 20-40 mJ pulse of 532 nm radiation generated from an Nd:YAG laser. The timing is such that the ablation plume is entrained into the expanding gas and then passes through two cylindrical copper electrodes separated by 1 cm and biased with a 700-900 V potential, which drives a 20-40 mA discharge current. The discharge increased the MgC<sub>4</sub>H and MgC<sub>3</sub>N yields by up to a factor of 5 relative to ablation alone likely due to the enhanced reactivity of electronically excited Mg\* atoms or Mg+ cations [30,31,39,40].

The rotational spectra were measured with a cavity FTMW spectrometer operating from 5 to 26 GHz [41,42]. The cavity is aligned co-axially with the supersonic expansion and surrounded by three pairs of Helmholtz coils tuned to cancel the Earth's magnetic field, which causes Zeeman splitting and shifts of the rotational transitions of openshell molecules. Residual magnetic fields near the cavity boundaries are estimated to be less than 50 mG, and the rest frequencies of the rotational transitions were measured to an accuracy of 2 kHz.

Using the spectroscopic parameters of putative MgC<sub>4</sub>H and MgC<sub>3</sub>N derived from astronomical observations (which span 30–110 GHz [13]), rest frequencies of both molecules in the 5–26 GHz bandwidth of the cavity spectrometer were predicted to an accuracy of 100 kHz, sufficiently small to be searched for at a single position of the microwave cavity, which has very high sensitivity but a narrow instantaneous bandwidth, i.e.  $< 0.5\,\mathrm{MHz}$ . Microwave features of both MgC<sub>4</sub>H and

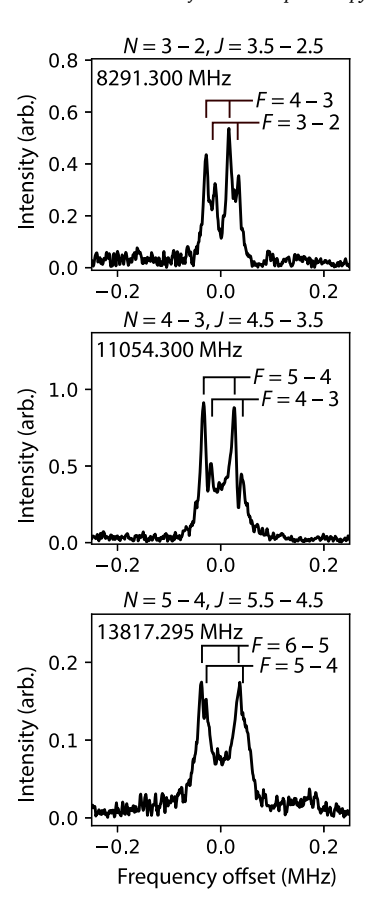


**Fig. 2.** Cavity FTMW measurements of MgC<sub>4</sub>H. The N and J quantum numbers are indicated above each panel, which is plotted with respect to the frequency offset from the center frequency shown. These transitions exhibit a larger Doppler splitting due to the co-axial cavity-expansion geometry and a smaller hyperfine splitting from the Fermi contact interaction of the H nuclear spin (I = 1/2). The hyperfine doublets are labeled by the total angular momentum quantum number F (F = I + J). From top to bottom, the spectra are the result of 7 min, 12 min, and 70 min of integration, respectively.

MgC<sub>3</sub>N were readily observed after optimizing the experimental conditions for the production of MgCCH. Various assays were then performed to better constrain the chemical composition and properties of these carriers. Both required the ablation laser to be on, indicating they contain magnesium. The MgC4H transitions were observed with both acetylene and diacetylene precursors, but with a larger signal intensity (up to a factor of 2) from the latter. The optimal concentration of either precursor was 0.15% in neon. The MgC<sub>3</sub>N transitions required the presence of acetonitrile as a nitrogen source. A 1:1 acetonitrile:acetylene mixture (both 0.08% in neon) optimized the MgC<sub>3</sub>N signal, which was slightly more intense than that without acetylene (i.e. a pure 0.08% acetonitrile precursor). Both MgC<sub>4</sub>H and MgC<sub>3</sub>N transitions were sensitive to applied magnetic fields, displaying characteristic Zeeman splittings when one of the Helmholtz coils was turned off, as expected for an open-shell molecule. By examining the dependence of the signal on the microwave excitation power, we estimated that MgC<sub>4</sub>H has a dipole moment comparable to MgCCH (calculated to be 2.3 D and 1.7 D, respectively [43,44]) and that MgC<sub>3</sub>N has a dipole moment comparable to MgNC (calculated and measured to be 6.4 D and 5.3 D, respectively [13,26]). Accounting for the dipole moments and molecular partition functions at the typical rotational temperature of 2 K in the expansion, we estimate MgC<sub>4</sub>H and MgC<sub>3</sub>N to be a factor of 10-100 less abundant than MgCCH and MgNC, respectively, at the ablation-discharge expansion conditions optimized for MgC<sub>4</sub>H/MgC<sub>3</sub>N production, as described above. It is worth noting that a prior attempt to produce MgC<sub>3</sub>N (and CaC<sub>3</sub>N) in another laboratory equipped with a similar laser ablation expansion source, but using BrC<sub>3</sub>N, IC<sub>3</sub>N, or HC<sub>3</sub>N precursors, resulted in no detectable rotational transitions [45]. As the authors of that study pointed out, a possible explanation in this instance is the formation of divalent  $M(C_3N)_2$  molecules instead, following thermochemical arguments. Given our own observations of MgCCH, MgNC, and MgC<sub>4</sub>H from HCCH, CH<sub>3</sub>CN, and HC<sub>4</sub>H precursors, respectively, we would expect MgC<sub>3</sub>N to be detectable in our source with an HC<sub>3</sub>N precursor, even with laser ablation alone (i.e. no discharge). Thus, it may also be the case that, despite comparable laser ablation pulse energies, the use of a picosecond pulse in the prior experiments (compared to the nanosecond pulses used here) might influence the population of  $Mg^*/Mg^+$  atoms, which appear to be important to the formation of monovalent alkaline earth metal-ligand molecules [40], or otherwise affect the precursor chemistry.

#### 3. Theoretical methods

The structural and electronic properties of MgC<sub>4</sub>H and MgC<sub>3</sub>N were computed with coupled-cluster quantum chemical methods in CFOUR [46,47]. The optimized geometries and first-order properties were calculated with analytic derivative techniques for coupled-cluster theory with single, double, and perturbative triple excitations [CCSD(T)] with both unrestricted (UHF) [48-50] and restricted openshell (ROHF) [51,52] reference wavefunctions and correlationconsistent polarized core-valence basis sets with double, triple, and quadruple  $\zeta$  functions (cc-pCVXZ, X = D, T, Q) [53–55]. All electrons except those occupying the inner-core Mg 1s orbital were correlated. As discussed further below, the quadratically convergent self-consistent field (QCSCF) code in CFOUR [56] was used to address inconsistent convergence of UHF solutions using a standard DIIS algorithm [57]. Vibrational zero-point corrections to the ground-state rotational constants were derived with second-order vibrational perturbation theory (VPT2) [58] using cubic force fields calculated by finite differences.

#### 4. Results

The laboratory rest frequencies of MgC<sub>4</sub>H and MgC<sub>3</sub>N are listed in Tables 1 and 2. Some examples of the measured line profiles for MgC<sub>4</sub>H are shown in Fig. 2. An effective Hamiltonian for a  ${}^2\Sigma$  electronic state including rotational (B), centrifugal distortion (D), spin-rotation  $(\gamma)$ , Fermi contact  $(b_E)$ , spin-dipole  $(c, MgC_3N \text{ only})$ , and electric quadrupole coupling (eOq, MgC<sub>3</sub>N only) parameters was fit to the measured lines using the SPFIT/SPCAT programs [59]. The small hyperfine parameters in MgC<sub>4</sub>H produced observable splittings only for transitions with  $N \leq 3$ , and its spectrum could be fit to the measurement uncertainty with a Fermi contact term only, fixing c = 0. MgC<sub>3</sub>N exhibits much larger hyperfine splittings at low N owing to the electric quadrupole moment of the  $^{14}N$  nucleus (I=1). The partial collapse of the quadrupole splitting at high N led to congestion of MgC<sub>3</sub>N transitions above 14 GHz, which were excluded from the laboratory analysis because the hyperfine-weighted line center could not be confidently determined (see Fig. 3). The spectroscopic parameters derived from a laboratory-only data set and a combined laboratory-astronomical data set incorporating the 30-110 GHz transitions reported in Ref. [13] are summarized in Table 3. Although the astronomical frequencies have much larger measurement uncertainties (0.1-1.0 MHz) than the laboratory frequencies (2 kHz), the higher frequency range of the former helps to reduce the uncertainties of the derived B and D parameters. The rest frequencies calculated with the combined fit parameters for the strongest transitions below 40 GHz have a predicted uncertainty of ~1-10 kHz. The raw line lists and fitting files are available in a permanent online data repository [60].

The optimized geometry and first-order electronic properties of MgC<sub>4</sub>H and MgC<sub>3</sub>N at the CCSD(T)/cc-pCVQZ level of theory are summarized in Table 4, which includes results for both UHF and ROHF reference wavefunctions. The  $\langle \hat{S}^2 \rangle$  expectation value of the UHF

Table 1
The laboratory rest frequencies of MgC<sub>4</sub>H.

N'	J'	F'	N	J	F	Frequency (MHz) <sup>a</sup>	Obs. – Calc. (kHz)
2	2.5	3	1	1.5	2	5 528.2833	0.7
3	2.5	3	2	1.5	2	8 286.7583	1.0
3	2.5	2	2	1.5	1	8 286.7812	2.8
3	3.5	4	2	2.5	3	8 291.2930	1.5
3	3.5	3	2	2.5	2	8 291.3098	-2.8
4	3.5	4	3	2.5	3	11 049.7634	-7.3
4	3.5	3	3	2.5	2	11 049.7818	-0.5
4	4.5	5	3	3.5	4	11 054.2951	-0.3
4	4.5	4	3	3.5	3	11 054.3074	0.4
5	4.5	5	4	3.5	4	13812.7767 <sup>b</sup>	4.5
5	4.5	4	4	3.5	3	13812.7767 <sup>b</sup>	-2.9
5	5.5	6	4	4.5	5	13817.2959 <sup>b</sup>	3.3
5	5.5	5	4	4.5	4	13817.2959 <sup>b</sup>	-4.1
6	5.5	6	5	4.5	5	16 575.7681 <sup>b</sup>	4.7
6	5.5	5	5	4.5	4	16 575.7681 <sup>b</sup>	-0.4
6	6.5	7	5	5.5	6	16 580.2859 <sup>b</sup>	4.3
6	6.5	6	5	5.5	5	16 580.2859 <sup>b</sup>	-0.8
7	6.5	7	6	5.5	6	19338.7484 <sup>b</sup>	4.7
7	6.5	6	6	5.5	5	19338.7484 <sup>b</sup>	0.9
7	7.5	8	6	6.5	7	19343.2618 <sup>b</sup>	1.2
7	7.5	7	6	6.5	6	19343.2618 <sup>b</sup>	-2.5
8	7.5	8	7	6.5	7	22 101.7115 <sup>b</sup>	-0.5
8	7.5	7	7	6.5	6	22 101.7115 <sup>b</sup>	-3.4
8	8.5	9	7	7.5	8	22 106.2289 <sup>b</sup>	1.0
8	8.5	8	7	7.5	7	22 106.2289 <sup>b</sup>	-1.9

<sup>&</sup>lt;sup>a</sup> The measurement uncertainty is 2 kHz.

Table 2
The laboratory rest frequencies of MgC N

The laboratory rest frequencies of MgC <sub>3</sub> N.								
N'	J'	F'	N	J	$\boldsymbol{F}$	Frequency (MHz) <sup>a</sup>	Obs Calc. (kHz)	
3	2.5	2.5	2	1.5	1.5	8 283.0704	2.0	
3	2.5	3.5	2	1.5	2.5	8 283.2305	0.8	
3	3.5	2.5	2	2.5	1.5	8 287.3963	1.3	
3	3.5	3.5	2	2.5	2.5	8 287.4446	0.6	
3	3.5	4.5	2	2.5	3.5	8 287.5473	-0.8	
4	3.5	2.5	3	2.5	1.5	11 044.8171	-0.4	
4	3.5	3.5	3	2.5	2.5	11 044.8722	-2.0	
4	3.5	4.5	3	2.5	3.5	11 044.9466	0.1	
4	4.5	3.5	3	3.5	2.5	11 049.2159	0.2	
4	4.5	4.5	3	3.5	3.5	11 049.2402	-1.8	
4	4.5	5.5	3	3.5	4.5	11 049.2966	-1.5	
5	4.5	4.5	4	3.5	3.5	13 806.6394	-3.7	
5	4.5	5.5	4	3.5	4.5	13 806.6873	3.4	
5	5.5	4.5	4	4.5	3.5	13 810.9914	-4.5	
5	5.5	5.5	4	4.5	4.5	13 811.0202	6.8	
5	5.5	6.5	4	4.5	5.5	13 811.0485	-0.1	

<sup>&</sup>lt;sup>a</sup> The measurement uncertainty is 2 kHz.

reference wavefunction is  $\sim$ 1.2 for both MgC<sub>4</sub>H and MgC<sub>3</sub>N, which is evidence of significant spin contamination that is only partly removed in the correlated wavefunction. (The exact value for a doublet state is 3/4.) The UHF and ROHF optimized bond lengths show differences of up to  $\sim$ 0.008 Å, while the difference in quantities that depend on the unpaired spin density are even more pronounced. For example, the UHF and ROHF predictions for the magnetic hyperfine coupling constants ( $b_F$  and c) for both H and <sup>14</sup>N differ substantially in absolute magnitude and sign. Molecular properties that depend on the total electron density such as the electric dipole moment and electric quadrupole coupling constant of <sup>14</sup>N exhibit much smaller UHF-ROHF differences.

In the course of this work, it was observed that two different UHF solutions could be converged depending on the choice of SCF algorithm (DIIS or QCSCF) and basis set. The results in Table 4 correspond to the spin-contaminated solution, which was always found by the QCSCF solver and appears to be the rigorous variational minimum. For MgC<sub>3</sub>N with the cc-pCV(D,T,Q)Z basis sets and MgC<sub>4</sub>H with the cc-pCV(D,T)Z basis sets, a conventional DIIS algorithm converged a weakly spin-contaminated solution  $(\langle \hat{S}^2 \rangle_{CC} - 3/4 < 10^{-3})$ . This weakly

<sup>&</sup>lt;sup>b</sup> Hyperfine splitting is unresolved. The mean transition frequency is reported.

Table 3 The spectroscopic constants of  $MgC_4H$  and  $MgC_7N$ .

Parameter		$MgC_4H$		MgC <sub>3</sub> N		
	Lab <sup>a</sup>	Astro <sup>b</sup>	Combined <sup>c</sup>	Lab <sup>a</sup>	Astro <sup>b</sup>	Combined <sup>c</sup>
В	1381.5071(1)	1381.512(4)	1381.50723(6)	1380.8873(2)	1380.888(1)	1380.88767(7)
$D \times 10^3$	0.069(12)	0.074(2)	0.0712(5)	0.067(5)	0.0760(5)	0.0760(3)
γ	4.513(1)	4.7(1)	4.513(1)	4.382(2)	4.35(4)	4.382(2)
$b_F$	0.91(9)	-	0.92(9)	-0.20(3)	_	-0.19(3)
c	[0.0]	-	[0.0]	0.56(6)	_	0.56(6)
eQq	-	-	-	-4.15(8)	-	-4.17(8)
$rms^d$	1.2	-	1.2	1.3	-	1.0
$N_{ m lines}{}^{ m e}$	17		34	16		57

Note — All values are given in MHz with  $1\sigma$  uncertainties in parentheses in units of the last digit.

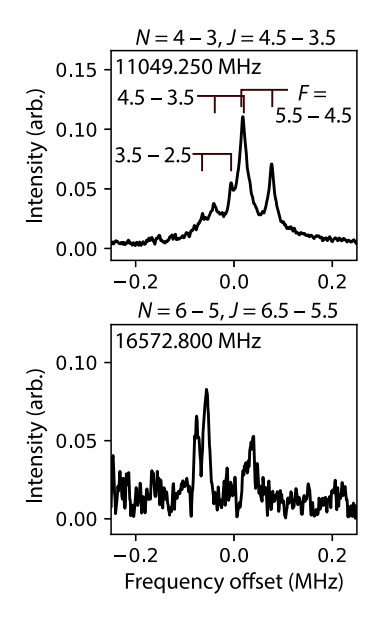
- <sup>a</sup> Laboratory data fitted only.
- <sup>b</sup> Astronomical parameters from Ref. [13].
- <sup>c</sup> Laboratory and astronomical data fitted together.
- <sup>d</sup> Dimensionless rms of the residuals normalized to their respective measurement uncertainties.
- <sup>e</sup> Number of independent transition frequencies included in the fit.

Table 4 Calculated properties of MgC<sub>4</sub>H and MgC<sub>3</sub>N.

Parameter	Mg	C <sub>4</sub> H	Mg	$MgC_3N$	
	UHF	ROHF	UHF	ROHF	
$r_{\mathrm{MgC}_1}/\mathring{\mathrm{A}}^{\mathrm{a}}$	2.04545	2.04425	2.06424	2.06273	
$r_{\mathrm{C_{1}C_{2}}}/\mathrm{\mathring{A}}$	1.22189	1.22975	1.21910	1.22679	
$r_{\mathrm{C}_2\mathrm{C}_3}/\mathrm{\mathring{A}}$	1.37979	1.37345	1.38310	1.37721	
$r_{\mathrm{C_3C_4/C_3N}}/\mathrm{\mathring{A}}$	1.20434	1.21147	1.15586	1.16256	
$r_{\mathrm{C_4H}}/\mathrm{\mathring{A}}$	1.06149	1.06171	-	-	
$B_e/\mathrm{MHz^b}$	1379.240	1376.409	1378.374	1375.641	
$\Delta B_{\rm vib}/{\rm MHz^b}$	-	2.445 <sup>b</sup>	-	$2.629^{b}$	
$\mu_e/a.u.^c$	0.841	0.834	2.518	2.494	
$\rho_{\mathrm{Mg}}/\mathrm{a.u.^d}$	0.99198	0.93520	1.06112	0.99916	
$\rho_{C_1}/a.u.$	0.10955	0.12629	0.10848	0.12546	
$\rho_{\rm C_2}/{\rm a.u.}$	0.04303	0.01695	0.04383	0.01705	
$\rho_{C_3}/a.u.$	-0.02659	0.00334	-0.02551	0.00305	
$\rho_{C_4/N}/a.u.$	0.02412	-0.00051	0.02044	-0.00055	
$\rho_{\rm H}/{\rm a.u.}$	-0.00387	0.00018	-	-	
$\langle \hat{S}^2 \rangle_{\text{SCF}}^{\mathbf{e}}$	1.196	0.750	1.161	0.750	
$\langle \hat{S}^2 \rangle_{\rm CC}$	0.815	0.750	0.806	0.750	
$b_F/{ m MHz^f}$	-17.277	0.803	6.595	-0.178	
c/MHz	6.640	0.053	-6.464	0.553	
$eQq/\mathrm{MHz}$	-	-	-4.305	-4.170	

 ${\it Note}$  — The optimized geometries and electronic properties were calculated at the UHF-or ROHF-CCSD(T)/cc-pCVQZ level of theory, except where otherwise noted.

contaminated UHF reference wavefunction yielded optimized CCSD(T) bond lengths that differed from the ROHF-CCSD(T) values by  $10^{-4}$  Å or less. Nonetheless, despite the similar optimized structures, the unpaired spin density of the weakly contaminated UHF-CCSD(T) wavefunction still differed substantially from that of the ROHF-CCSD(T) wavefunction. The values of the  $b_F$  and c parameters of MgC<sub>3</sub>N with the former, for example, were 1.426 MHz and 2.157 MHz, respectively, which are considerably larger than the ROHF predictions in Table 4. (The weakly spin contaminated UHF solution could not be found for MgC<sub>4</sub>H with the cc-pCVQZ basis set.)



**Fig. 3.** Cavity FTMW measurements of MgC<sub>3</sub>N. The center frequencies and (N, J, F) quantum numbers are labeled as in Fig. 2. Each spin-rotation transition is split into three <sup>14</sup>N nuclear hyperfine components (I = 1), which are incompletely resolved (and unassigned) for transitions above 14 GHz. The top and bottom spectra are the result of 130 min and 230 min of integration, respectively.

#### 5. Discussion

The combined laboratory, theoretical, and astronomical evidence unambiguously confirms the identification of  $MgC_4H$  and  $MgC_5N$  in IRC+10216 by Cernicharo et al. [13]. The next longer chains,  $MgC_6H$  and  $MgC_5N$ , have also been detected by radio astronomy in this source [14]. If the  $MgCCH:MgC_4H \approx 10^1:1-10^2:1$  abundance ratio in our laser ablation-electric discharge holds for  $MgC_4H:MgC_6H$  (and similarly for  $MgC_5N$ ), then it should be possible to detect both of the longer species at similar experimental conditions, particularly as the laboratory rest frequencies in the cm-wave band can be predicted with relatively small uncertainties («1 MHz) using the astronomically derived spectroscopic constants.

The structural and electronic properties of MgC<sub>4</sub>H and MgC<sub>3</sub>N demonstrate that their ionic metal-carbon bonding is very similar to that of their smaller chain analogues. Although the lack of isotopic data prevents a complete structural analysis at this juncture, if we constrain all bond lengths other than the Mg–C bond to their optimized ROHF-CCSD(T)/cc-pCVQZ values, then the semi-experimental equilibrium rotational constants,  $B_{\rm sc} = B_0 - \Delta B_{\rm vib}$ , derived from

 $<sup>^{</sup>a}$  The bond lengths with  $C_1$ ,  $C_2$ , etc., labeling the C atoms beginning with that closest to Mg.

 $<sup>^{</sup>m b}$   $B_e$  is the equilibrium rotational constant.  $\Delta B_{
m vib} = B_0 - B_e$  is the zero-point vibrational correction. The  $\Delta B_{
m vib}$  values were calculated with VPT2 using the cc-pCVTZ basis set.

<sup>&</sup>lt;sup>c</sup> The equilibrium electric dipole moment.

<sup>&</sup>lt;sup>d</sup> The unpaired spin densities evaluated at sequential nuclei.

 $<sup>^{\</sup>rm e}$   $\langle \hat{S}^2 \rangle_{\rm SCF}$  is the SCF expectation value of  $\hat{S}^2$ , and  $\langle \hat{S}^2 \rangle_{\rm CC}$  is the projected expectation value  $\langle 0 | \hat{S}^2 \exp(\hat{T}) | 0 \rangle$ , where  $\hat{T}$  is the coupled-cluster excitation operator.

 $<sup>^{\</sup>rm f}$   $b_F$  and c are the Fermi contact and spin-dipole hyperfine coupling constants for  ${
m H}/{
m ^{14}N}$ . eQq is the electric quadrupole coupling constant for  $^{14}{
m N}$ .

the measured  $B_0$  values and theoretical vibrational corrections (Table 4) imply that the semi-experimental equilibrium metal-carbon bond lengths are  $r_{\rm se}({\rm Mg-C_4H})\approx 2.039\,{\rm \mathring{A}}$  and  $r_{\rm se}({\rm Mg-C_3N})\approx 2.057\,{\rm \mathring{A}}$ . These are similar to the Mg-C bond length in MgCCH ( $r_{\rm se}=2.0369(7)\,{\rm \mathring{A}}$  [30]) and somewhat shorter than that in MgCN (~2.072  ${\rm \mathring{A}}$  [32,61]). In the (usually very good) approximation that the spin-rotation constants ( $\gamma$ ) are dominated by second-order spin-orbit contributions [62], the ratio  $\gamma/B$  can also be compared between different Mg-bearing chain molecules to assess changes between the electronic state manifold of the unpaired  $\sigma(sp)$  electron centered on the Mg atom. The  $\gamma/B$  values of MgC<sub>4</sub>H and MgC<sub>3</sub>N are  $3.27\times 10^{-3}$  and  $3.17\times 10^{-3}$ , respectively, while the values for MgCCH and MgCN are  $3.36\times 10^{-3}$  [29–31] and  $2.95\times 10^{-3}$  [32]. The small spread (~10%) of these ratios illustrates that the unpaired Mg-centered electron in each of these molecules experiences a similar electronic environment.

The strong localization of the unpaired electron is also reflected by the small magnitude of the magnetic hyperfine parameters of the H and N nuclei, which are farthest from the Mg radical center. The good agreement between the calculated ROHF-CCSD(T) hyperfine parameters and the measured  $b_F(H)$ ,  $b_F(N)$ , and c(N) values highlights the importance of beginning with a ROHF determinant and the high sensitivity of these properties to even small amounts of spin contamination. The unpaired spin densities at each nucleus, reported in Table 4, decay approximately exponentially with distance from the Mg atom, a pattern similar to that observed experimentally in isotopologues of MgCCH, CaCCH, and SrCCH [30]. This behavior bolsters the idea that biradical electronic interactions in  $M-(C\equiv C)_n-M'$  chains can potentially be tuned over several orders of magnitude by varying the number of C2 linker units. Controlling this coupling will have an important influence on the optical cycling properties of hypermetallic polyatomic molecules for next-generation laser-cooling applications [37,38].

#### 6. Conclusions

The linear magnesium-carbon chains  $MgC_4H$  and  $MgC_3N$  were detected and characterized at high-resolution in the laboratory by cavity FTMW spectroscopy. A parallel quantum chemical analysis highlighted the influence of spin contamination on accurate predictions of their structural and magnetic hyperfine parameters. This study lays the foundation for a number of follow-up investigations targeting their substituted isotopic species, positively and negatively charged ions, and hypermetallic derivatives. The characterization of these molecules will provide the spectroscopic data needed to critically assess the chemical evolution of metal-carbon chains in astrophysical environments and the suitability of their unique electronic structure for applications in fundamental molecular physics.

## CRediT authorship contribution statement

P. Bryan Changala: Writing – review & editing, Writing – original draft, Visualization, Validation, Project administration, Methodology, Investigation, Funding acquisition, Formal analysis, Conceptualization. Nadav Genossar-Dan: Writing – review & editing, Validation, Investigation, Formal analysis, Conceptualization. Joshua H. Baraban: Writing – review & editing, Validation, Supervision, Project administration, Funding acquisition, Formal analysis, Conceptualization. Michael C. McCarthy: Writing – review & editing, Supervision, Project administration, Funding acquisition, Conceptualization.

### Declaration of competing interest

The authors declare that they have no known competing financial interests or personal relationships that could have appeared to influence the work reported in this paper.

#### Data availability

Data will be made available on request.

#### Acknowledgments

The authors thank Prof. John F. Stanton (University of Florida) for helpful discussions regarding spin contamination. This work was supported by the U.S. National Science Foundation Award Nos. PHY-2110489 and AST-1908576, and by the U.S.-Israel Binational Science Foundation (Grant No. 2020724). N.G.-D. and J.H.B. are also supported by the Israel Science Foundation (ISF), Grant No. 194/20. N.G.-D. acknowledges the VATAT scholarship for Ph.D. students in quantum science and technology.

#### References

- B.E. Turner, T.C. Steimle, L. Meerts, Detection of sodium cyanide (NaCN) in IRC 10216, Astrophys. J. Lett. 426 (1994) L97, http://dx.doi.org/10.1086/174043, URL https://ui.adsabs.harvard.edu/abs/1994ApJ...426L...97T/abstract.
- [2] M. Guélin, S. Muller, J. Cernicharo, A.J. Apponi, M.C. McCarthy, C.A. Gottlieb, P. Thaddeus, Astronomical detection of the free radical SiCN, Astron. Astrophys. 363 (2000) L9.
- [3] L.M. Ziurys, C. Savage, J.L. Highberger, A.J. Apponi, M. Guélin, J. Cernicharo, More metal cyanide species: Detection of AlNC (X¹Σ⁺) toward IRC+10216, Astrophys. J. 564 (2002) L45, http://dx.doi.org/10.1086/338775, URL https://ui.adsabs.harvard.edu/abs/2002ApJ...564L..45Z/abstract.
- [4] M. Guélin, S. Muller, J. Cernicharo, M.C. McCarthy, P. Thaddeus, Detection of the SiNC radical in IRC+10216, Astron. Astrophys. 426 (2004) L49, http: //dx.doi.org/10.1051/0004-6361:200400074.
- [5] R.L. Pulliam, C. Savage, M. Agúndez, J. Cernicharo, M. Guélin, L.M. Ziurys, Identification of KCN in IRC+10216: Evidence for selective cyanide chemistry, Astrophys. J. Lett. 725 (2010) L181, http://dx.doi.org/10.1088/2041-8205/725/ 2/L181, URL https://ui.adsabs.harvard.edu/abs/2010ApJ...725L.181P/abstract.
- [6] L.N. Zack, D.T. Halfen, L.M. Ziurys, Detection of FeCN (X<sup>4</sup>Δ<sub>i</sub>) in IRC+10216: A new interstellar molecule, Astrophys. J. Lett. 733 (2011) L36, http://dx.doi.org/10.1088/2041-8205/733/2/L36.
- [7] C. Cabezas, J. Cernicharo, J.L. Alonso, M. Agundez, S. Mata, M. Guelin, I. Peña, Laboratory and astronomical discovery of hydromagnesium isocyanide, Astrophys. J. 775 (2013) 133, http://dx.doi.org/10.1088/0004-637X/775/2/133, URL http://arxiv.org/abs/1309.0371.
- [8] M. Agúndez, J. Cernicharo, M. Guélin, New molecules in IRC+10216: confirmation of C<sub>5</sub>S and tentative identification of MgCCH, NCCP, and SiH<sub>3</sub>CN, Astron. Astrophys. 570 (2014) A45, http://dx.doi.org/10.1051/0004-6361/201424542, URL http://arxiv.org/abs/1408.6306.
- [9] J. Cernicharo, L. Velilla-Prieto, M. Agúndez, J.R. Pardo, J.P. Fonfría, G. Quintana-Lacaci, C. Cabezas, C. Bermúdez, M. Guélin, Discovery of the first Ca-bearing molecule in space: CaNC, Astron. Astrophys. 627 (2019) L4, http://dx.doi.org/ 10.1051/0004-6361/201936040.
- [10] C. Cabezas, J.R. Pardo, M. Agúndez, B. Tercero, N. Marcelino, Y. Endo, P. de Vicente, M. Guélin, J. Cernicharo, Discovery of two metallic cyanoacetylides in IRC+10216: HMgCCCN and NaCCCN, Astron. Astrophys. 672 (2023) L12, http://dx.doi.org/10.1051/0004-6361/202346462.
- [11] K. Kawaguchi, E. Kagi, T. Hirano, S. Takano, S. Saito, Laboratory spectroscopy of MgNC: The first radioastronomical identification of Mg-bearing molecule, Astrophys. J. Lett. 406 (1993) L39, http://dx.doi.org/10.1086/186781, URL https://ui.adsabs.harvard.edu/abs/1993ApJ...406L..39K/abstract.
- [12] L.M. Ziurys, A.J. Apponi, M. Guelin, J. Cernicharo, Detection of MgCN in IRC+10216: A new metal-bearing free radical, Astrophys. J. 445 (1995) L47, http://dx.doi.org/10.1086/187886.
- [13] J. Cernicharo, C. Cabezas, J.R. Pardo, M. Agúndez, C. Bermúdez, L. Velilla-Prieto, F. Tercero, J.A. López-Pérez, J.D. Gallego, J.P. Fonfría, G. Quintana-Lacaci, M. Guélin, Y. Endo, Discovery of two new magnesium-bearing species in IRC+10216: MgC<sub>3</sub>N and MgC<sub>4</sub>H, Astron. Astrophys. 630 (2019) L2, http://dx.doi.org/10.1051/0004-6361/201936372, URL https://www.aanda.org/10.1051/0004-6361/201936372.
- [14] J.R. Pardo, C. Cabezas, J.P. Fonfría, M. Agúndez, B. Tercero, P. De Vicente, M. Guélin, J. Cernicharo, Magnesium radicals  $MgC_5N$  and  $MgC_6H$  in IRC+10216, Astron. Astrophys. 652 (2021) L13, http://dx.doi.org/10.1051/0004-6361/202141671.
- [15] J. Cernicharo, C. Cabezas, J.R. Pardo, M. Agúndez, O. Roncero, B. Tercero, N. Marcelino, M. Guélin, Y. Endo, P. de Vicente, The magnesium paradigm in IRC +10216: Discovery of MgC<sub>4</sub>H<sup>+</sup>, MgC<sub>3</sub>N<sup>+</sup>, MgC<sub>6</sub>H<sup>+</sup>, and MgC<sub>5</sub>N<sup>+</sup>, Astron. Astrophys. 672 (2023) L13, http://dx.doi.org/10.1051/0004-6361/202346467, URL https://www.aanda.org/10.1051/0004-6361/202346467.

- [16] P.B. Changala, H. Gupta, J. Cernicharo, J.R. Pardo, M. Agúndez, C. Cabezas, B. Tercero, M. Guélin, M.C. McCarthy, Laboratory and astronomical discovery of magnesium dicarbide, MgC<sub>2</sub>, Astrophys. J. Lett. 940 (2022) L42, http://dx.doi.org/10.3847/2041-8213/aca144, URL https://iopscience.iop.org/article/10.3847/2041-8213/aca144.
- [17] R.C. Dunbar, S. Petrie, Interstellar and circumstellar reaction kinetics of Na<sup>+</sup>, Mg<sup>+</sup>, and Al<sup>+</sup> with cyanopolyynes and polyynes, Astrophys. J. 564 (2002) 792, http://dx.doi.org/10.1086/324196, URL https://ui.adsabs.harvard.edu/abs/2002ApJ...564..792D/abstract.
- [18] S. Petrie, On the formation of metal cyanides and related compounds in the circumstellar envelope of IRC+10216, Mon. Not. R. Astron. Soc. 282 (1996) 807–819, http://dx.doi.org/10.1093/MNRAS/282.3.807, URL https://ui.adsabs. harvard.edu/abs/1996MNRAS.282..807P/abstract.
- [19] S. Petrie, R.C. Dunbar, Radiative association reactions of Na<sup>+</sup>, Mg<sup>+</sup>, and Al<sup>+</sup> with abundant interstellar molecules. variational transition state theory calculations, J. Phys. Chem. A 104 (2000) 4480–4488, http://dx.doi.org/10.1021/jp993485q, URL https://pubs.acs.org/doi/10.1021/jp993485q.
- [20] G.K. Corlett, A.M. Little, A.M. Ellis, LIF spectroscopy of the MgCCH free radical, Chem. Phys. Lett. 249 (1996) 53–58, http://dx.doi.org/10.1016/0009-2614(95) 01364-4
- [22] D.W. Tokaryk, A.G. Adam, W.S. Hopkins, High-resolution laser spectroscopy of the  $\tilde{A}^2\Pi$   $\tilde{X}^2\Sigma^+$  transition of MgCCH, J. Mol. Spectrosc. 230 (2005) 54–61, http://dx.doi.org/10.1016/j.jms.2004.10.008.
- [23] E. Chasovskikh, E.B. Jochnowitz, J.P. Maier, Electronic spectra of the  $MgC_4H$  and  $MgC_6H$  radicals, J. Phys. Chem. A 112 (37) (2008) 8686–8689, http://dx.doi.org/10.1021/jp803969a, URL https://pubs.acs.org/doi/abs/10.1021/jp803969a.
- [24] H. Ding, C. Apetrei, Ł. Chacaga, J.P. Maier, Electronic spectra of MgC<sub>2n</sub>H (n=1-3) chains in the gas phase, Astrophys. J. 677 (2008) 348–352, http://dx.doi.org/10.1086/524375, URL https://iopscience.iop.org/article/10.1086/524375. https://iopscience.iop.org/article/10.1086/524375/meta.
- [25] D. Forthomme, C. Linton, D.W. Tokaryk, A.G. Adam, A.D. Granger, High-resolution laser spectroscopy of the Ā<sup>2</sup>Π X̄<sup>2</sup>Σ+ transition of MgC<sub>4</sub>H, Chem. Phys. Lett. 488 (4–6) (2010) 116–120, http://dx.doi.org/10.1016/j.cplett.2010.
- [26] T.C. Steimle, R.R. Bousquet, The permanent electric dipole moment of MgNC, J. Chem. Phys. 115 (2001) 5203, http://dx.doi.org/10.1063/1.1396853, URL https://aip.scitation.org/doi/abs/10.1063/1.1396853.
- [27] M. Fukushima, T. Ishiwata, The  $\nu_2$  bending vibrational structure of the  $\tilde{X}^2\Sigma^+$  state of MgNC, J. Chem. Phys. 135 (2011) 124311, http://dx.doi.org/10.1063/1.3640024, URL https://aip.scitation.org/doi/abs/10.1063/1.3640024.
- [28] M.A. Anderson, L.M. Ziurys, Laboratory detection and millimeter spectrum of the MgCCH radical, Astrophys. J. 439 (1995) L25, http://dx.doi.org/10.1086/ 187736
- [29] M. Brewster, A. Apponi, J. Xin, L. Ziurys, Millimeter-wave spectroscopy of vibrationally-excited NaCCH ( $\tilde{X}^1\Sigma^+$ ) and MgCCH ( $\tilde{X}^2\Sigma^+$ ): the  $\nu_5$  bending mode, Chem. Phys. Lett. 310 (1999) 411-422, http://dx.doi.org/10.1016/S0009-2614(99)00816-7, URL https://www.sciencedirect.com/science/article/pii/S0009261499008167.
- [30] P.B. Changala, N. Genossar-Dan, E. Brudner, T. Gur, J.H. Baraban, M.C. Mc-Carthy, Structural and electronic trends of optical cycling centers in polyatomic molecules revealed by microwave spectroscopy of MgCCH, CaCCH, and SrCCH, Proc. Natl. Acad. Sci. 120 (28) (2023) e2303586120, http://dx.doi.org/10.1073/pnas.2303586120, URL https://pnas.org/doi/10.1073/pnas.2303586120.
- [31] J.E. Burns, Q. Cheng, R.C. Fortenberry, M. Sun, L.N. Zack, T. Zaveri, N.J. DeYonker, L.M. Ziurys, A computational and spectroscopic study of MgCCH ( $X^2\Sigma^+$ : towards characterizing MgCCH $^+$ , Mol. Phys. (2023) http://dx.doi.org/10.1080/00268976.2023.2267135, URL https://www.tandfonline.com/doi/full/10.1080/00268976.2023.2267135.
- [32] M.A. Anderson, T.C. Steimle, L.M. Ziurys, M.A. Anderson, T.C. Steimle, L.M. Ziurys, The millimeter and submillimeter rotational spectrum of the MgCN radical ( $X^2 \Sigma^+$ ), Astrophys. J. Lett. 429 (1994) L41, http://dx.doi.org/10.1086/187408, URL https://ui.adsabs.harvard.edu/abs/1994ApJ...429L..41A/abstract.
- [33] M.A. Anderson, L.M. Ziurys, The millimeter-wave spectrum of  $^{25}$ MgNC and  $^{26}$ MgNC: bonding in magnesium isocyanides, Chem. Phys. Lett. 231 (1994) 164–170, http://dx.doi.org/10.1016/0009-2614(94)01259-8.
- [34] K.A. Walker, M.C. Gerry, <sup>14</sup>N hyperfine structure in the pure rotational spectrum of <sup>24</sup>Mg<sup>14</sup>N<sup>12</sup>C, J. Mol. Spectrosc. 189 (1998) 40–45, http://dx.doi.org/10.1006/ JMSP.1997.7515.
- [35] T.A. Isaev, R. Berger, Polyatomic candidates for cooling of molecules with lasers from simple theoretical concepts, Phys. Rev. Lett. 116 (2016) 063006, http:// dx.doi.org/10.1103/PhysRevLett.116.063006, URL https://link.aps.org/doi/10. 1103/PhysRevLett.116.063006.
- [36] I. Kozyryev, L. Baum, K. Matsuda, J.M. Doyle, Proposal for laser cooling of complex polyatomic molecules, ChemPhysChem 17 (2016) 3641–3648, http:// dx.doi.org/10.1002/cphc.201601051, URL http://doi.wiley.com/10.1002/cphc. 201601051.

- [37] M.J. O'Rourke, N.R. Hutzler, Hypermetallic polar molecules for precision measurements, Phys. Rev. A 100 (2019) 022502, http://dx.doi.org/10.1103/PhysRevA.100.022502, URL https://journals.aps.org/pra/abstract/10.1103/PhysRevA.100.022502.
- [38] M.V. Ivanov, S. Gulania, A.I. Krylov, Two cycling centers in one molecule: Communication by through-bond interactions and entanglement of the unpaired electrons, J. Phys. Chem. Lett. 11 (2020) 1297–1304, http://dx.doi.org/10.1021/ acs.jpclett.0c00021, URL https://pubs.acs.org/doi/10.1021/acs.jpclett.0c00021.
- [39] M. Sun, D.T. Halfen, J. Min, B. Harris, D.J. Clouthier, L.M. Ziurys, The rotational spectrum of CuCCH(X<sup>1</sup>Σ\*): A Fourier transform microwave discharge assisted laser ablation spectroscopy and millimeter/submillimeter study, J. Chem. Phys. 133 (2010) 174301, http://dx.doi.org/10.1063/1.3493690, URL https://aip.scitation.org/doi/abs/10.1063/1.3493690.
- [40] P.F. Bernath, Spectroscopy and photochemistry of polyatomic alkaline earth containing molecules, Adv. Photochem. 23 (1997) 1–62, http://dx.doi.org/10. 1002/9780470133545.ch1, URL https://onlinelibrary.wiley.com/doi/10.1002/ 9780470133545.ch1
- [41] J.U. Grabow, E.S. Palmer, M.C. McCarthy, P. Thaddeus, Supersonic-jet cryogenic-resonator coaxially oriented beam-resonator arrangement Fourier transform microwave spectrometer, Rev. Sci. Instrum. 76 (2005) 093106, http://dx.doi.org/10.1063/1.2039347, URL http://aip.scitation.org/doi/10.1063/1.2039347.
- [42] K.N. Crabtree, M.-A. Martin-Drumel, G.G. Brown, S.A. Gaster, T.M. Hall, M.C. McCarthy, Microwave spectral taxonomy: A semi-automated combination of chirped-pulse and cavity Fourier-transform microwave spectroscopy, J. Chem. Phys. 144 (2016) 124201, http://dx.doi.org/10.1063/1.4944072, URL http://scitation.aip.org/content/aip/journal/jcp/144/12/10.1063/1.4944072.
- [43] I. Bâldea, Profiling astrophysically relevant MgC<sub>4</sub>H chains. An attempt to aid astronomical observations, Mon. Not. R. Astron. Soc. 498 (2020) 4316–4326, http://dx.doi.org/10.1093/mnras/staa2354, URL https://academic.oup.com/mnras/article/498/3/4316/5903288.
- [44] D.E. Woon, Ab initio characterization of MgCCH, MgCCH<sup>+</sup>, and MgC<sub>2</sub> and pathways to their formation in the interstellar medium, Astrophys. J. 456 (1996) 602, http://dx.doi.org/10.1086/176682, URL https://ui.adsabs.harvard.edu/abs/1996ApJ...456..602W/abstract. http://adsabs.harvard.edu/doi/10.1086/176682.
- [45] C. Cabezas, C. Barrientos, A. Largo, J.-C. Guillemin, J. Cernicharo, J.L. Alonso, Alkaline and alkaline-earth cyanoacetylides: A combined theoretical and rotational spectroscopic investigation, J. Chem. Phys. 151 (2019) http://dx.doi.org/10.1063/1.5110670, URL https://pubs.aip.org/jcp/article/151/5/054312/198725/Alkaline-and-alkaline-earth-cyanoacetylides-A.
- [46] J.F. Stanton, J. Gauss, L. Cheng, M.E. Harding, D.A. Matthews, P.G. Szalay, CFOUR, coupled-cluster techniques for computational chemistry, a quantum-chemical program package, 2020.
- [47] D.A. Matthews, L. Cheng, M.E. Harding, F. Lipparini, S. Stopkowicz, T.-C. Jagau, P.G. Szalay, J. Gauss, J.F. Stanton, Coupled-cluster techniques for computational chemistry: The cfour program package, J. Chem. Phys. 152 (2020) 214108, http://dx.doi.org/10.1063/5.0004837, URL http://aip.scitation.org/doi/10.1063/5.0004837.
- [48] K. Raghavachari, G.W. Trucks, J.A. Pople, M. Head-Gordon, A fifth-order perturbation comparison of electron correlation theories, Chem. Phys. Lett. 157 (1989) 479–483, http://dx.doi.org/10.1016/S0009-2614(89)87395-6.
- [49] R.J. Bartlett, J. Watts, S. Kucharski, J. Noga, Non-iterative fifth-order triple and quadruple excitation energy corrections in correlated methods, Chem. Phys. Lett. 165 (1990) 513–522, http://dx.doi.org/10.1016/0009-2614(90)87031-L, URL https://linkinghub.elsevier.com/retrieve/pii/000926149087031L.
- [50] J.D. Watts, J. Gauss, R.J. Bartlett, Open-shell analytical energy gradients for triple excitation many-body, coupled-cluster methods: Mbpt(4), CCSD+T(CCSD), CCSD(T), and QCISD(T), Chem. Phys. Lett. 200 (1992) 1–7, http://dx.doi.org/ 10.1016/0009-2614(92)87036-O, URL https://linkinghub.elsevier.com/retrieve/ pii/000926149287036O.
- [51] J. Gauss, W.J. Lauderdale, J.F. Stanton, J.D. Watts, R.J. Bartlett, Analytic energy gradients for open-shell coupled-cluster singles and doubles (CCSD) calculations using restricted open-shell Hartree—Fock (ROHF) reference functions, Chem. Phys. Lett. 182 (1991) 207, http://dx.doi.org/10.1016/0009-2614(91)80203-A, URL https://linkinghub.elsevier.com/retrieve/pii/0009261491802034.
- [52] J.D. Watts, J. Gauss, R.J. Bartlett, Coupled-cluster methods with noniterative triple excitations for restricted open-shell Hartree-Fock and other general single determinant reference functions. Energies and analytical gradients, J. Chem. Phys. 98 (1993) 8718, http://dx.doi.org/10.1063/1.464480, URL http://aip. scitation.org/doi/10.1063/1.464480.
- [53] T.H. Dunning, Gaussian basis sets for use in correlated molecular calculations. I. The atoms boron through neon and hydrogen, J. Chem. Phys. 90 (1989) 1007, http://dx.doi.org/10.1063/1.456153, URL http://scitation.aip.org/content/aip/journal/jcp/90/2/10.1063/1.456153.
- [54] D.E. Woon, T.H. Dunning, Gaussian basis sets for use in correlated molecular calculations. V. Core-valence basis sets for boron through neon, J. Chem. Phys. 103 (1995) 4572–4585, http://dx.doi.org/10.1063/1.470645, URL http://aip. scitation.org/doi/10.1063/1.470645.
- [55] B.P. Prascher, D.E. Woon, K.A. Peterson, T.H. Dunning, A.K. Wilson, Gaussian basis sets for use in correlated molecular calculations. VII. Valence, core-valence, and scalar relativistic basis sets for Li, Be, Na, and Mg, Theor. Chem. Acc.

- 128 (2011) 69–82, http://dx.doi.org/10.1007/S00214-010-0764-0, URL https://link.springer.com/article/10.1007/s00214-010-0764-0.
- [56] T. Nottoli, J. Gauss, F. Lipparini, A black-box, general purpose quadratic self-consistent field code with and without Cholesky decomposition of the twoelectron integrals, Mol. Phys. 119 (21–22) (2021) http://dx.doi.org/10.1080/ 00268976.2021.1974590, URL https://www.tandfonline.com/doi/full/10.1080/ 00268976.2021.1974590.
- [57] P. Pulay, Improved SCF convergence acceleration, J. Comput. Chem. 3 (1982) 556–560, http://dx.doi.org/10.1002/jcc.540030413, URL https://onlinelibrary. wiley.com/doi/10.1002/jcc.540030413.
- [58] I.M. Mills, Vibration-rotation structure in asymmetric- and symmetric-top molecules, in: K.N. Rao, C.W. Mathews (Eds.), Molecular Spectroscopy: Modern Research, Academic Press, New York, 1972, pp. 115–140, Ch. 3.2.
- [59] H.M. Pickett, The fitting and prediction of vibration-rotation spectra with spin interactions, J. Mol. Spectrosc. 148 (1991) 371–377, http://dx.doi.org/10.1016/ 0022-2852(91)90393-0.
- [60] P.B. Changala, N. Genossar-Dan, J.H. Baraban, M.C. McCarthy, Data for "laboratory rotational spectroscopy of the magnesium-carbon chains  $MgC_4H$  and  $MgC_3N$ ", 2024, http://dx.doi.org/10.5281/zenodo.10779111.
- [61] T. Hirano, K. Ishii, T.E. Odaka, P. Jensen, A theoretical study of MgNC and MgCN in the  $\bar{X}^2\Sigma^+$  electronic state, J. Mol. Spectrosc. 215 (2002) 42–57, http://dx. doi.org/10.1006/jmsp.2002.8598, URL https://linkinghub.elsevier.com/retrieve/pii/S002228520298598X.
- [62] A.J. Stone, Gauge invariance of the g tensor, Proc. Roy. Soc. A 271 (1963) 424–434, http://dx.doi.org/10.1098/rspa.1963.0027, URL https://royalsocietypublishing.org/doi/10.1098/rspa.1963.0027.